RESEARCH ACTIVITIES III
Department of Electronic Structure

III-A Synthesis and Characterization of Exotic Molecule Based Nano-Crystals of Metal Acetylides: Toward Carbon Encapsulated Metal Dot Array, Metal Nano-Networks and Metal-Carbon Hybrid Systems

Metal-carbon binary junctions are expected to exhibit interesting properties, such as Shottoky barrier rectification, optical and tunneling devices, and chemical protector against oxidation. Metal acetylides have the ionic bond between the metallic cation and the acetylide anion. In the simplest case, divalent metal cations (M^{2+}) form a fcc lattice structure with a C_2^{2-} anion between the two metal cations. The introduction of alkyl or aromatic group into the C_2 unit, producing $R–C{\equiv}C^-$, can generate organometallic cluster compounds $((R–C{\equiv}C^-)_aM^{a+})_n$, ($a$ = 1, 2), some of which can be isolated as single crystals. These cluster compounds are soluble in organic solvent and provide solid films with nano-scale planarity by spin-coating method. Photoexcitation of metal-acetylides induces charge-neutralization reaction producing carbon-skinned metal particles, metallic nanowires or nano-sheets covered with organic polymer matrices. This property leads us to apply for photo-lithographical pattern generation of metallic circuits or magnetic arrays. On the other hand, the reaction mechanism of the photoreactions of the respective acetylide systems can be highly dependent on the electronic structure of metal atoms. We are also illuminating the mechanism of these reactions.

III-A-1 Self-Assembled Nanowire Synthesis of Highly-Anisotropic Copper Acetylide Molecules

JUDAI, Ken; NISHIJO, Junichi; OKABE, Chie; NISHI, Nobuyuki

Various methods have been suggested for metallic and semiconductive nanowire production, template based synthesis, vapor-liquid-solid growth, solution-liquid-solid process, oxide-assisted growth and so on. Above all, the production using a highly anisotropic crystal can be regarded as due to self-assembly of small molecules or atoms to a nanowire. The self-assembly method has potential advantage of relatively low cost, high purity, and large-scale production. However, only limited materials have anisotropic properties, for example, molybdenum chalcogenides, selenium, and tellurium. Besides, it is very hard to produce thin nanowires by only highly anisotropic properties. Here we report a new compound having a highly anisotropic crystal structure. Copper acetylide (C_2Cu_2) molecules self-assemble into ultra thin nanowires under an extremely slow nucleation condition. Moreover, annealing of the C_2Cu_2 nanowires converts to copper nanocables encapsulated in carbon outer layers. The copper nanocable core is extremely thin, in which only 8 Cu atoms can line up in the diameter.

One of the merits of self-assembly nanowire production is an extremely simple procedure of just preparing only a building block. The C_2Cu_2 nanowire can be also generated facilely. Figure 1 shows a scanning electron microscopy (SEM) image of C_2Cu_2 products on silicon substrates, where the C_2Cu_2 suspension in methanol has been dropped onto and air-dried. Nanowire morphology was observed when the C_2H_2 exposing rate was kept extremely slow (0.05 mL/min). Although C_2Cu_2 was synthesized by chemical reaction of gram-order production in a flask, microscopic shape of the product is a nanoscale needle-like crystal. This indicates that C_2Cu_2 molecules aggregate and self-assemble into nanowire morphology in an aqueous solution. On the contrary to the successful production of nanowires, a fast exposing rate of C_2H_2 gas gave amorphous products. The key step of self-assembling for the nano-structure is just only the control of the nucleation rate of acetylide molecules.

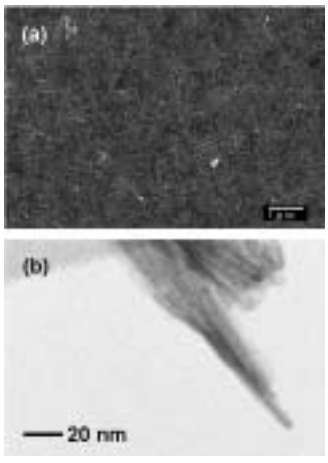

Figure 1. (a) SEM image of C_2Cu_2 precipitate. Nanowire morphology can be obtained in the extremely slow nucleation condition. (b) TEM image of an end of a budle of C_2Cu_2 wires.

III-A-2 Photochemical Conversion of (Cu^+ $C{\equiv}C^-$-*t*-Butyl)$_{24}$ Cluster Molecules to Cu Metallic Nano-Sheets Embedded in Polymer Nano-Film

NISHI, Nobuyuki; NISHIJO, Junichi; OKABE, Chie; OISHI, Osamu; JUDAI, Ken

Only a limited number of the cluster molecules with more than 20 metal atoms is known as structure-analyzed clusters. Olblich *et al.* reported the synthetic method and X-ray diffraction analysis of (Cu^+ $C{\equiv}C^-$-*t*-Butyl)$_{24}$ in1993. This molecule is soluble and show red emission in *n*-hexane but its electronic absorption spectrum exhibits concentration dependence originated from molecular association. The association occurs in the concentration higher than 1×10^{-4} M. The spectral pattern of the thin film of this molecule is essentially the same as that of 1×10^{-3} M solution of *n*-hexane, showing a peak at 228 nm and a shoulder at 282 nm The absorption threshold is seen at 510 nm. This absorption feature is essentially the same as those of monomer or dimer species of similar complex molecules. Cluster formation changes little of the electronic structure indicating very weak metal-metal interactions in these multinuclear cluster molecules. From the analogy of similar systems of various coordinated copper clusters, the emission is believed to originate from the triplet metal-ethynyl charge transfer state rather localized in a single pair. No emission is seen from the thin films and one can expect the presence of radiationless pathways for heat generation or reaction channel(s). The UV absorption spectrum of the spin-coated film shows a peak at 232 nm and a shoulder 282 nm that is accompanied with the tail at 400 nm to 520 nm and the broad absorption (or background) down to near infrared region. The last broad extension is believed due to the optical scattering characteristics of the thin film. Thus, the photoexcitation of the film is expected to cause energy transfer in the triplet state. This molecule has 24 Cu-ethynyl groups and intracluster T-T annihilation can be induced. The infrared spectrum of the film also changes upon photoexcitation. The original cluster shows a doublet band at 1455 and 1474 cm^{-1} characteristic of the coupled two -C≡C$^-$ bonds. On the photo-illumination, new bands appear at higher frequencies, 1552 and 1573 cm^{-1}. This indicates that the charge neutralization produces strong double bond networks around metallic copper fragments. Figure 1 shows the Transmission Electron Microscope (TEM) images of the film heated at 250 °C (left) and that irradiated with UV light from a 500W high pressure mercury lamp. The heating produces Cu nanoparticles with spherical or polyhedral shapes. The dominant sizes of the particles are 3.3 nm, 5.2 nm, 7 nm, 10.5 nm and 14 nm, suggesting the growth due to particle joining. On the other hand, photoexcitation causes growth of cubic crystals or planer copper sheets joining together and extending the metallic area wider and wider. Since the photoexcitation puts the energy into the metal atoms rather predominantly, the neutralized metal atoms are thought to cohere in the original crystal planes where the Cu cations are located. The heating may excites both metal atoms and organic parts simultaneously and allow the metal atoms cohere three dimentionally.

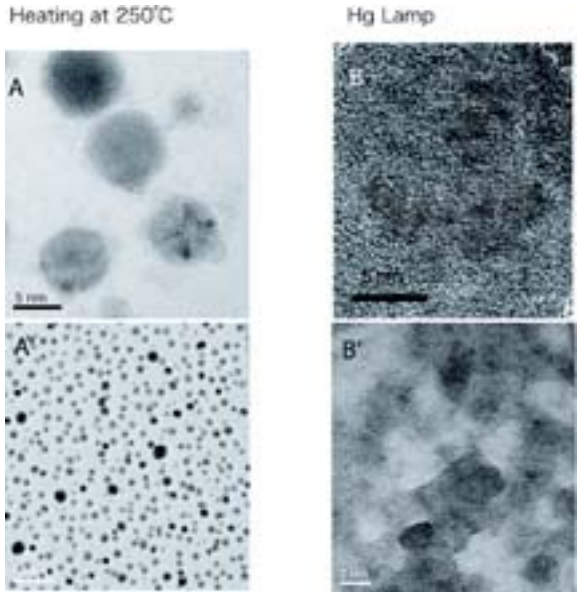

Figure 1. High resolution TEM images of heated (left; A and A') and photoexcited (right; B and B') (Cu^+ $C{\equiv}C^-$-*t*-Butyl)$_{24}$ cluster films on collodion membranes.

III-A-3 Guest Controlled Magnetism of CoC_2 Nanoparticles

NISHIJO, Junichi; JUDAI, Ken; NISHI, Nobuyuki

The structure of molecule-based magnets is often affected by gas or solvent absorption owing to their flexibility, and the flexibility opens up the way for controlling their magnetism by a chemical environment. We discovered that the molecule-based magnet CoC_2 is an outstanding example of the "controllable magnet."

The as-prepared anhydrous CoC_2 shows superparamagnetic behavior down to 2.5 K with the Curie constant of C = 2.5 emu K/mol and saturation magnetization of M_S = 1.5 μ_B. Below 2.5 K, a small part of anhydrous CoC_2 shows ferromagnetic (FM) behavior, but the major part of anhydrous CoC_2 are still superparamagnetic. The large Curie constant indicates the short range strong FM interaction between Co^{2+} cations. Though the existence of strong FM interactions, orientation disorder of the C_2^{2-} brings the weakening of the interaction in many places and prevents the FM transition. Once the material is exposed to ammonia gas, the CoC_2 absorbs ammonia molecules accompanied by orientation ordering of the C_2^{2-}. The orientation ordering also means that the strength of the interaction between spins tend to be uniform. Indeed, the increase in the Curie constant from 2.5 to 3.5 emu K/mol by ammonia absorption suggests that the area of short range FM ordering is expanded by absorption, while the M_S keeps same value. The absorbed ammonia molecules are easily desorbed under ammonia-free condition. The desorption lowers the Curie constant from 3.5 to 2.7 emu K/mol. The decrease of the Curie constant is explained by the partial orientation disorder of C_2^{2-}; that

is, desorption process disturbs the orientation of C_2^{2-} again, which reduces the range of the FM short range ordering. After the 1st absorption/desorption cycle, the Curie constant changes reversibly from 3.2 to 2.7 emu K/mol for ammonia absorbed and desorbed CoC_2, respectively.

The field-cooled (FC, 10 Oe) and zero field-cooled (ZFC) susceptibilities for ammonia absorbed and desorbed CoC_2 are shown in figure 1. The 1st absorption raises both FC susceptibility and blocking temperature of T_B = 20 K, which is indicated by the peak of ZFC susceptibility. Desorption lowers ZFC susceptibility and T_B, but the values are still larger than those of anhydrous CoC_2. After the 1st absorption/desorption cycle, though the ZFC susceptibility and T_B of ammonia absorbed CoC_2 is little smaller than that of 1st cycle, the magnetism changes reversibly by absorption and desorption of ammonia. The T_B and the ZFC susceptibility at 1.8 K are raised from 5 K and 7.5 emu/mol to 10 K and 17 emu/mol, respectively, by ammonia absorption.

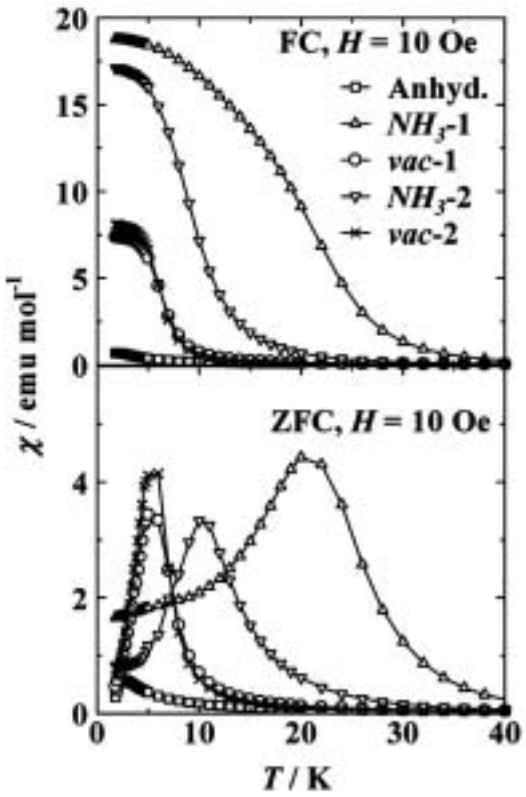

Figure 1. Field-cooled (FC) and zero field-cooled (ZFC) susceptibilities of ammonia absorbed/desorbed CoC_2. The legends *NH_3*-i and *vac*-i indicate the i-th times ammonia.

III-A-4 Formation of Carbon-Encapsulated Metallic Nano-Particles from Metal Acetylides by Electron Beam Irradiation

NISHIJO, Junichi; OKABE, Chie; BUSHIRI, Junaid M.; KOSUGI, Kentaroh; NISHI, Nobuyuki; SAWA, Hiroshi

[*Eur. Phys. J. D* **34**, 219–222 (2005)]

Transition metal acetylides, MC_2 (M = Fe, Co and Ni), exhibit ferromagnetic behavior of which T_C is characteristic of their size and structure. CoC_2 synthesized in anhydrous condition exhibited cubic structure with disordered C_2^{2-} orientation. Once being exposed to water (or air), the particles behave ferromagnetically due to the lengthening of the Co–Co distance by the coordination of water molecules to Co^{2+} cations. Heating of these particles induces segregation of metallic cores with carbon mantles. Electron beam or 193 nm laser beam can produce nanoparticles with metallic cores covered with carbon mantles.

III-A-5 Reexamination of the Structures and Energies of Li_2C_2 and Li_4C_4

LEE, Sang-Yeon[1]; BOO, Bong-Hyun[2]; KANG, Heun-Kag[2]; KANG, Dongeun[2]; JUDAI, Ken; NISHIJO, Junichi; NISHI, Nobuyuki
([1]Kyungpook Natl. Univ.; [2]Chungnam Natl. Univ.)

[*Chem. Phys. Lett.* **411**, 484–491 (2005)]

The structures and energies of Li_2C_2 and Li_4C_4 have been reexamined by DFT and MP2 methods using a variety of basis sets of 6-311+G(3df) and cc-pVXZ(X = T,Q,5). Two low-lying isomers are found as the local minima on the potential energy surfaces of Li_4C_4. The lowest energy structure is shown to be multiply bridged D_{2h} form. A newly found quadruply bridged C_i form is found to be a local minimum, lying in energy above D_{2h} form by 22 kJ/mol in the energy. Also the energetics of high-lying isomers such as tetralithiotetrahedrane isomers were evaluated and discussed.

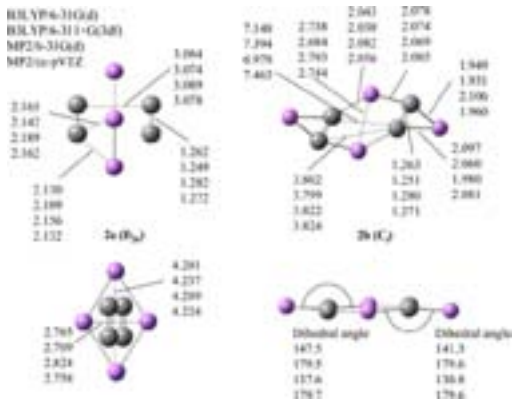

Figure 1. Geometries of low-lying isomers of Li_4C_4 optimized by the various methods indicated herein.

III-B Ultrafast Dynamics and Scanning Tunneling Microscopy

Proton transfer and geometrical isomerization processes in electronic excited states are investigated with our pico-femto dual wavelength valuable systems. For the study of molecules on metallic or crystalline surface, very low temperature Scanning Tunneling Microscope (LT STM) system are now in use for collaboration with users in universities.

III-B-1 Excited-State Double-Proton Transfer in the 7-Azaindole Dimer in Gas Phase 3. Reaction Mechanism Studied by Picosecond Time-Resolved REMPI Spectroscopy

SAKOTA, Kenji[1]; OKABE, Chie; NISHI, Nobuyuki; SEKIYA, Hiroshi[1]
([1]Kyushu Univ.)

[*J. Phys. Chem. A* **109**, 5245–5247 (2005)]

The excited state double-proton transfer (ESDPT) reaction in the jet-cooled 7-azaindole dimer ($7AI_2$) has been investigated with the picosecond time-resolved resonance-enhanced multiphoton ionization spectroscopy. The observed decay profiles of $7AI_2$ by exciting the origin and the intermolecular stretch fundamental in the S_1 state are well reproduced by single exponential functions with time constants of 1.9±0.9 ps and 860± 300 fs, respectively. This result provides a clear evidence of the concerted mechanism of ESDPT in $7AI_2$.

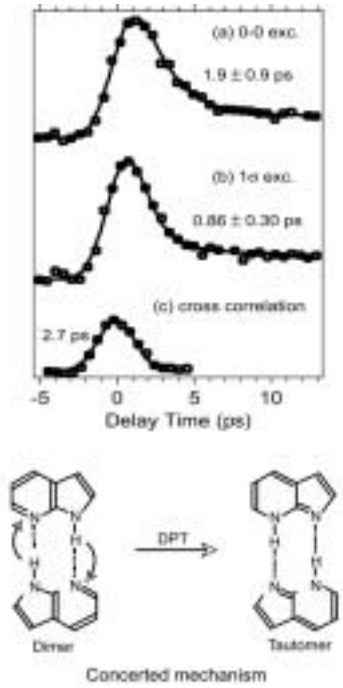

Figure 1. Top: Decay profiles of $7AI_2$ pumped at (a) the origin and (b) the intermolecular stretching band, respectively. The wavelength of the probe laser was fixed at 620 nm in (a) and (b). The open circles are experimental data, while the solid curves are best-fitted curves obtained by biexponential functions. The cross correlation trace is also indicated in (c). The instrumental time resolution given by the fwhm of the cross-correlation trace is 2.7 ps.
Bottom: Scheme of concerted mechanism.

III-B-2 Ultrafast Excited-State Dynamics in Photochromic *N*-Salicylideneaniline Studied by Femtosecond Time-Resolved REMPI Spectroscopy

OKABE, Chie; NAKABAYASHI, Takakazu[1]; INOKUCHI, Yoshiya; NISHI, Nobuyuki; SEKIYA, Hiroshi[2]
([1]Hokkaido Univ.; [2]Kyushu Univ.)

[*J. Chem. Phys.* **121**, 9436–9422 (2004)]

Ultrafast processes in photoexcited *N*-salicylideneaniline have been investigated with femtosecond time-resolved resonance-enhanced multiphoton ionization spectroscopy. The ion signals *via* the $S_1(n,\pi^*)$ state of the enol form as well as the proton-transferred *cis*-keto form emerge within a few hundred femtoseconds after photoexcitation to the first $S_1(\pi,\pi^*)$ state of the enol form. This reveals that two ultrafast processes, excited-state intramolecular proton transfer (ESIPT) reaction and an internal conversion (IC) to the $S_1(n,\pi^*)$ state, occur on a time scale less than a few hundred femtoseconds from the $S_1(\pi,\pi^*)$ state of the enol form. The rise time of the transient corresponding to the production of the proton-transferred *cis*-keto form is within 750 fs when near the red edge of the absorption is excited, indicating that the ESIPT reaction occurs within 750 fs. The decay time of the $S_1(\pi,\pi^*)$ state of the *cis*-keto form is 8.9 ps by exciting the enol form at 370 nm, but it dramatically decreases to be 1.5–1.6 ps for the excitation at 365–320 nm. The decrease in the decay time has been attributed to the opening of an efficient nonradiative channel; an IC from $S_1(\pi,\pi^*)$ to $S_1(n,\pi^*)$ of the *cis*-keto form promotes the production of the *trans*-keto form as the final photochromic products. The two IC processes may provide opposite effect on the quantum yield of photochromic products: IC in the enol form may substantially reduce the quantum yield, but IC in the *cis*-keto form increase it.

III-B-3 Orientation of Nitrous Oxide on Palladium(1 1 0) by STM

WATANABE, Kazuo[1]; KOKALJ, Anton[2]; INOKUCHI, Yoshiya[1]; RZEZNICKA, Izabela[3]; OHSHIMO, Keijiro; NISHI, Nobuyuki; MATSUSHIMA, Tatsuo[3]
([1]Univ. Tokyo; [2]J. Stefan Inst.; [3]Hokkaido Univ.)

[*Chem. Phys. Lett.* **406**, 474–478 (2005)]

The adsorption structure of N_2O on Pd(110) was analyzed below 14 K by scanning-tunneling microscopy. The N_2O monomer was oriented along the [001]

direction in the on-top form. Furthermore, the formation of small aggregates extending along the direction was observed. The observed images were well-simulated for two types of cluster structures optimized by density-functional theory calculations. The components in the aggregates are proposed to be in a tilted form either on bridge sites or on-top sites.

III-C Spectroscopic and Dynamical Studies of Molecular Cluster Ions

Electron defficiency of molecular cluster cations can attract electron rich groups or atoms exhibiting charge transfer or charge resonance interaction in the clusters. This causes dynamical structural change such as proton transfer or ion-core switching in hot cluster ions or clusters in solution.

III-C-1 Infrared Photodissociation Spectra and Solvation Structure of $Mg^+(CH_3OH)_n$ (n = 1–4)

MACHINAGA, Hironobu[1]; OHASHI, Kazuhiko[1]; INOKUCHI, Yoshiya[2]; NISHI, Nobuyuki; SEKIYA, Hiroshi[1]
([1]Kyushu Univ.; [2]Univ. Tokyo)

[*Chem. Phys. Lett.* **391**, 85–90 (2004)]

The infrared photodissociation spectra of mass-selected $Mg^+(CH_3OH)_n$ (n = 1–4) are measured and analyzed with the aid of density functional theory calculations. Hydrogen bonding between methanol molecules is found to be absent in $Mg^+(CH_3OH)_3$, but detected in $Mg^+(CH_3OH)_4$ through characteristic frequency shifts of the OH stretch of methanol. The maximum number of the methanol molecules that can be directly bonded to the Mg^+ ion is limited to three and the fourth molecule starts to fill the second solvation shell. The vibrational spectroscopy provides clear evidence for the closure of the first shell at n = 3.

III-C-2 Infrared Photodissociation Spectroscopy of $Mg^+(NH_3)_n$ (n = 3–6): Direct Coordination or Solvation through Hydrogen Bonding

OHASHI, Kazuhiko[1]; TERABARU, Kazutaka[1]; INOKUCHI, Yoshiya[2]; MUNE, Yutaka[1]; MACHINAGA, Hironobu[1]; NISHI, Nobuyuki; SEKIYA, Hiroshi[1]
([1]Kyushu Univ.; [2]Univ. Tokyo)

[*Chem. Phys. Lett.* **393**, 264–270 (2004)]

The infrared photodissociation spectra of mass-selected $Mg^+(NH_3)_n$ (n = 3–6) are measured and analyzed with the aid of density functional theory calculations. No large frequency reduction is observed for the NH stretches of ammonia, suggesting that either all the ammonia molecules coordinate directly to the Mg^+ ion or an additional ammonia in the second shell bridges two ammonias in the first shell through hydrogen bonds. Four or possibly five ammonia molecules are allowed to occupy the first shell, in striking contrast to the closure of the first shell in $Mg^+(H_2O)_3$.

III-C-3 Electronic Spectra of Jet-Cooled 3-Methyl-7-Azaindole Dimer. Symmetry of the Lowest Excited Electronic State and Double-Proton Transfer

HARA, Akihiko[1]; KOMOTO, Yusuke[1]; SAKOTA, Kenji[1]; MIYOSHI, Riko[1]; INOKUCHI, Yoshiya; OHASHI, Kazuhiko[1]; KUBO, Kanji[1]; YAMAMOTO, Emi[1]; MORI, Akira[1]; NISHI, Nobuyuki; SEKIYA, Hiroshi[1]
([1]Kyushu Univ.)

[*J. Phys. Chem. A* **108**, 10789–10793 (2004)]

The fluorescence excitation spectra are recorded for jet-cooled dual hydrogen-bonded 3-methyl-7-azaindole dimer $(3MAI)_2$-*hh* and deuterated dimers $(3MAI)_2$-*hd* and $(3MAI)_2$-*dd* near the electronic origin region of the S_1–S_0 transition, where *hd* and *dd* indicate the deuteration of an imino hydrogen and two imino hydrogens, respectively. A single origin is detected in the spectra of $(3MAI)_2$-*hh* and $(3MAI)_2$-*dd*, whereas two electronic origins separated by 13 cm^{-1} are detected in the spectrum of $(3MAI)_2$-*hd*. The excited-state double-proton transfer (ESDPT) occurs in $(3MAI)_2$-*hh*, while $(3MAI)_2$-*hd* and $(3MAI)_2$-*dd* undergo excited-state proton/deuteron transfer and excited-state double deuteron transfer, respectively. In $(3MAI)_2$-*hd*, the excitation is localized on either the 3MAI-*h* or 3MAI-*d* moiety. The localization of the excitation is explained by a weak coupling of the excitonic states of $(3MAI)_2$-*hh* and $(3MAI)_2$-*dd*. The effective symmetry of the lowest excited state of $(3MAI)_2$-*hh* and $(3MAI)_2$-*dd* belongs to the C_{2h} point group, while that of $(3MAI)_2$-*hd* belongs to the C_s point group. The vibronic patterns in the excitation spectra of the $(3MAI)_2$ dimers is very similar to those of the 7-azaindole dimers, indicating that the methyl substitution provides little effect on the shape of the ESDPT potential.

III-C-4 Structures of $[(CO_2)_n(H_2O)_m]^-$ (n = 1–4, m = 1, 2) Cluster Anions. I. Infrared Photodissociation Spectroscopy

MURAOKA, Azusa[1]; INOKUCHI, Yoshiya[1]; NISHI, Nobuyuki; NAGATA, Takashi[1]
([1]Univ. Tokyo)

[*J. Chem. Phys.* **122**, 094303 (7 pages) (2004)]

The infrared photodissociation spectra of $[(CO_2)_n(H_2O)_m]^-$ (n = 1–4, m = 1, 2) are measured in the 3000–3800 cm^{-1} range. The $[(CO_2)_n(H_2O)_1]^-$ spectra are characterized by a sharp band around 3570 cm^{-1} except for n = 1; $[(CO_2)_1(H_2O)_1]^-$ does not photodissociate in the spectral range studied. The $[(CO_2)_n(H_2O)_2]^-$ (n = 1, 2) species have similar spectral features with a broadband at 3340 cm^{-1}. A drastic change in the spectral features is observed for $[(CO_2)_3(H_2O)_2]^-$, where sharp bands appear at 3224, 3321, 3364, 3438, and 3572 cm^{-1}. *Ab initio* calculations are performed at the MP2/6-311++G** level to provide structural information such as optimized structures, stabilization energies, and vibrational frequencies of the $[(CO_2)_n(H_2O)_m]^-$ species. Comparison between the experimental and theoretical results reveals rather size- and composition-specific hydration manner in $[(CO_2)_n(H_2O)_m]^-$: (1) the incorporated H_2O is bonded to either CO_2^- or $C_2O_4^-$ through two equivalent OH···O hydrogen bonds to form a ring structure in $[(CO_2)_n(H_2O)_1]^-$; (2) two H_2O molecules are independently bound to the O atoms of CO_2^- in $[(CO_2)_n(H_2O)_2]^-$ (n = 1, 2); (3) a cyclic structure composed of CO_2^- and two H_2O molecules is formed in $[(CO_2)_3(H_2O)_2]^-$.